MANCHESTER 1824
The University of Manchester

Celebrating our bicentenary 200 years of education and innovation
Making a difference SINCE 1824 200 YEARS

Studying the Low-Z coast of the Island of Inversion: Exploring Two-Neutron Halos in N = 20 and N = 28 Isotones

Jagjit Singh

jagjit.singh@manchester.ac.uk

04.12.2024 (11:30-12:15)

DE LA RECHERCHE À L'INDUSTRIE
cea
ESNT
Espace de Structure Nucléaire Théorique
DSM - DAM

Light Nuclei Workshop
CEA Paris-Saclay
2024

Light nuclei between single-particle and clustering features

Introduction: 2n-halos (Borromean's)

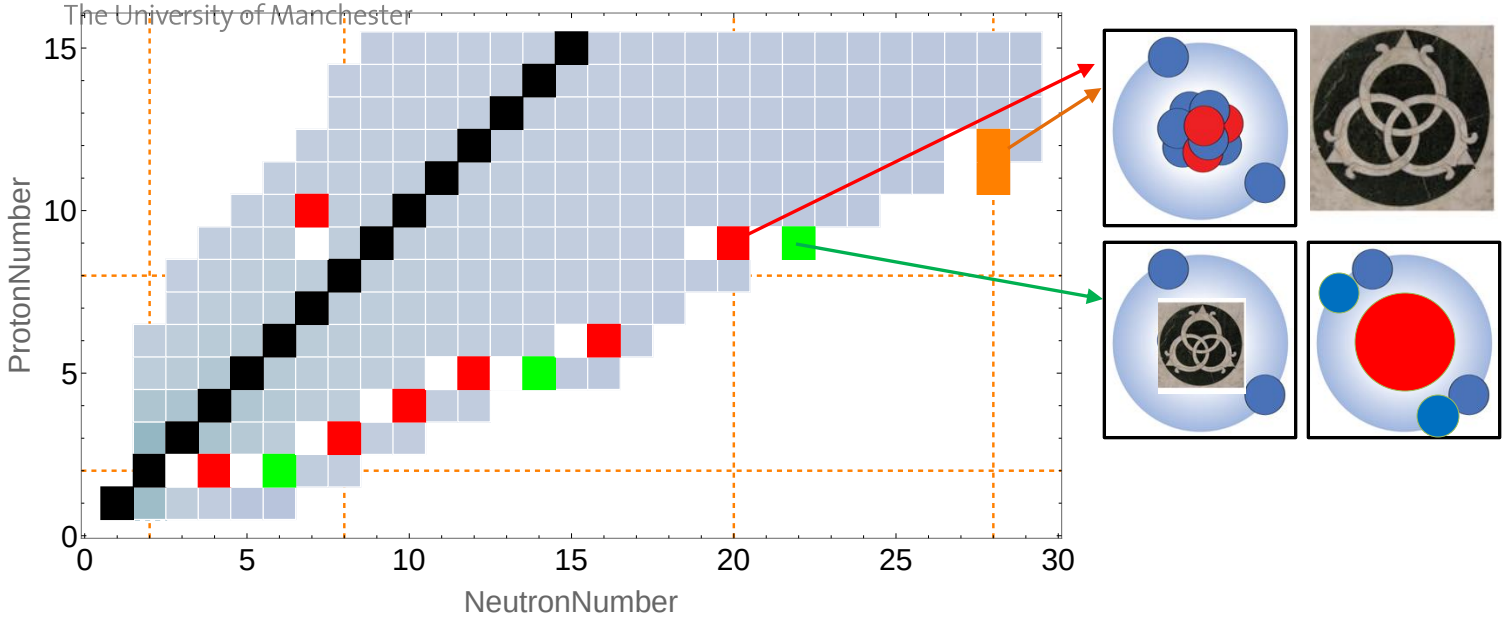

Key features of Borromean nuclei :

- Corresponding subsystems are unbound.
- Low two neucleon *separation energies* ($s_{2n/p}$).
- Diffuse *matter density distribution.*
- Abnormally large *matter radius.*
- Large *reaction/interaction cross sections.*
- Strong *correlations* between the valence neutrons are key in binding two-neutron halos.
- Enhanced *low-lying E1 strength.*

M. Zhukov et. al., Phys. Rep. ***231****, 151 (1993).*
P. G. Hansen and B. Jonson, Europhys. Lett. ***4****, 409 (1987).*
K. Hagino and H. Sagawa, PRC ***72****, 044321 (2005).*
M. Matsuo, PRC ***73****, 044309 (2006).*
A. Gezerlis, PRC ***81****, 025803 (2010).*
Y. Kikuchi et al., PTEP ***2016****, 103D03 (2016).*
T. Aumann, EPJA ***55****, 234 (2019).*

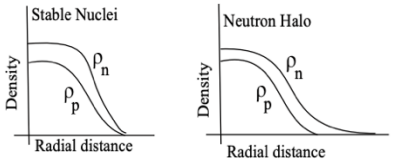

R. Kanungo, Handbook of Nuclear Physics (2023).

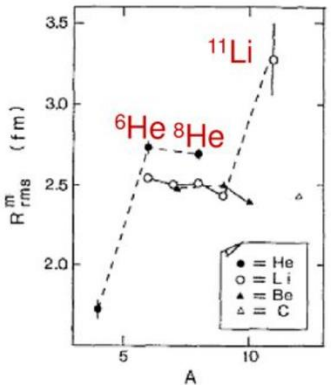

I. Tanihata et al., PRC ***55****, 2676 (1985) . PLB* ***160****, 380 (1985).*

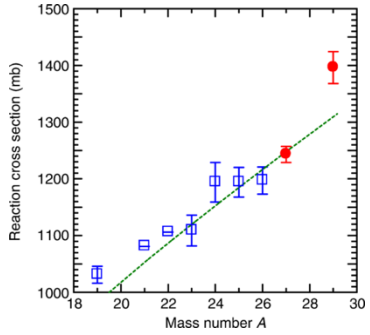

S. Bagchi et al., PRL ***124****, 222504 (2020).*

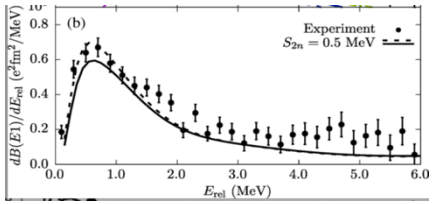

K. Cook et. al., PRL ***124****, 212503 (2020).*

Theoretically three-body (*core+n+n*) models describe reasonably well these features in *Borromean nuclei*.

Key inputs for these models are:

- Information on *core+n* low-lying spectrum
- Two-neutron separation energy.

JS, *PhD thesis, University of Padova (2016).*
J. Casal, Ph.D. thesis, Universidad de Sevilla (2016).

Current Experimental Status of 2n-halos (Borromean's)

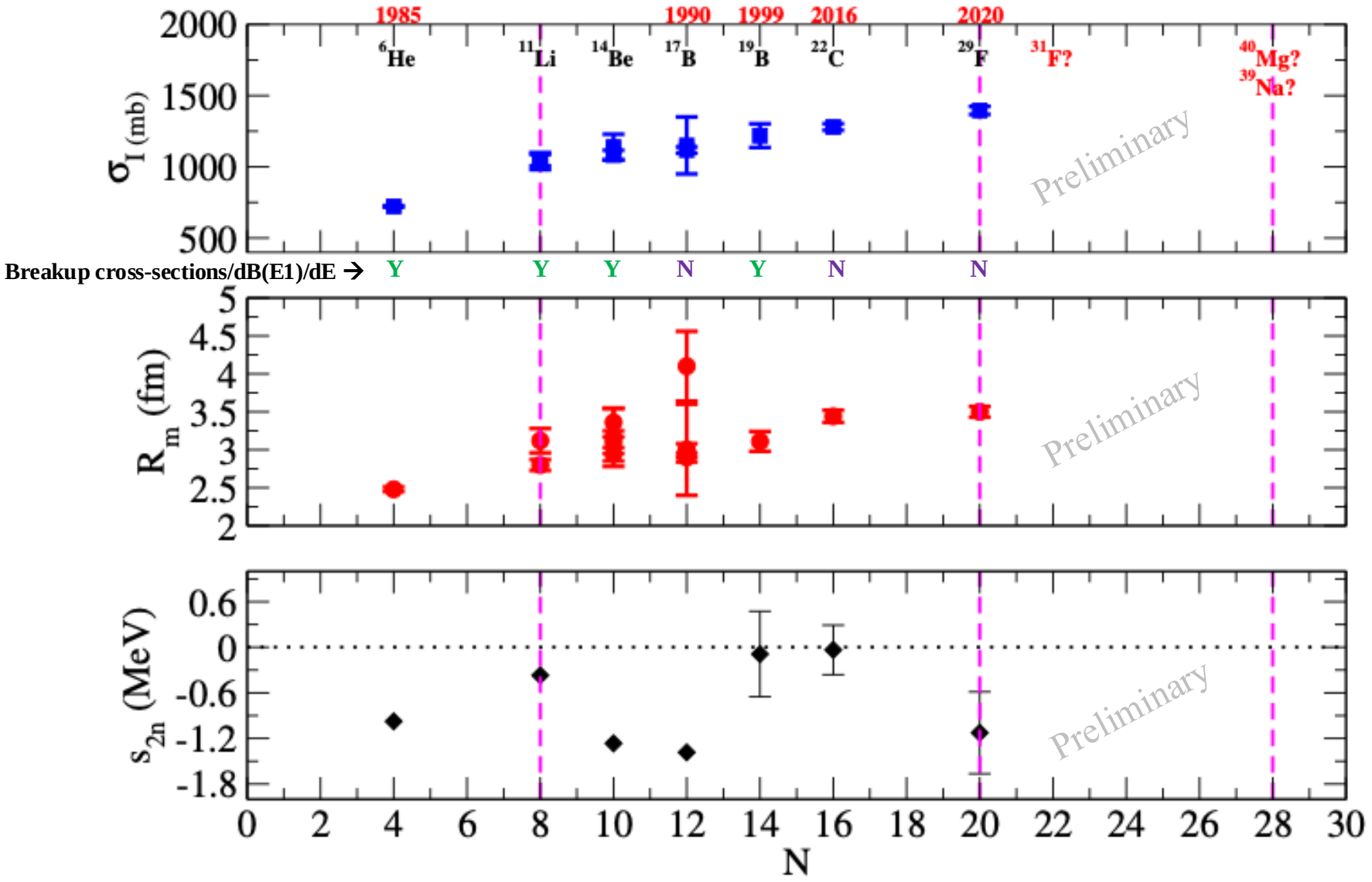

- *Tanihata et al., PRL **55**, 2676 (1985).*
- *I. Tanihata et al., in: W.D. Meyers, J.M. Nischke, E.B. Norman (Eds.), Radioactive Nuclear Beams, World Scientific, p. 429, (1990).*
- *T. Suzuki et al., Nucl. Phys. A **658,** 313 (1999).*
- *A. Ozawa et al., Nuclear Physics A **693** , 32 (2001).*
- *Y. Togano et al., Phys. Lett. B **761**, 412 (2016).*
- *S. Bagchi et al., PRL **124**, 222504 (2020).*
- *AME 2021: M. Wang et. al., CPC **45** (3) 030003 (2021).*

- *T. Aumann, et al., Phys. Rev. C **59**, 1252 (1999).*
- *J. Wang, et al., Phys. Rev. C **65**, 034306 (2002).*
- *T. Nakamura, et al., PRL **96,** 252502 (2006).*
- *K. Cook et. al., PRL **124**, 212503 (2020).*
- *Y. Sun et. al., PLB, **814**, 136072 (2021).*

^{31}F:

- *N. Michel et, al., PRC **101,** 031301(R) (2020).*
- *H. Masui et. al., PRC **101**, 041303(R) (2020)*
- *GS, **JS**, et al., PRC **105**, 014328 (2022).*

^{40}Mg

- *T. Baumann et. al., Nature 449, 1022 (2007).*
- *H. Crawford et. al., PRL **122,** 052501 (2019).*

^{39}Na

- *K. Y. Zhang et. al., PRC **107** (2023) L041303,*
- *D. S. Ahn et al., PRL **129**, 212502 (2022).*

2n-halo formation on lower Z-side of the magic numbers N=20 and 28

MANCHESTER 1824
The University of Manchester

^{33}Si	^{34}Si	^{35}Si	^{36}Si	^{37}Si	^{38}Si	^{39}Si	^{40}Si	^{41}Si	^{42}Si	^{43}Si	^{44}Si	^{45}Si
^{32}Al	^{33}Al	^{34}Al	^{35}Al	^{36}Al	^{37}Al	^{38}Al	^{39}Al	^{40}Al	^{41}Al	^{42}Al	^{43}Al	
^{31}Mg	^{32}Mg	^{33}Mg	^{34}Mg	^{35}Mg	^{36}Mg	^{37}Mg	^{38}Mg	^{39}Mg	^{40}Mg	^{41}Mg		
^{30}Na	^{31}Na	^{32}Na	^{33}Na	^{34}Na	^{35}Na	^{36}Na	^{37}Na	^{38}Na	^{39}Na			
^{29}Ne	^{30}Ne	^{31}Ne	^{32}Ne	^{33}Ne	^{34}Ne							
^{28}F	^{29}F	^{30}F	^{31}F									

N=28

N=20

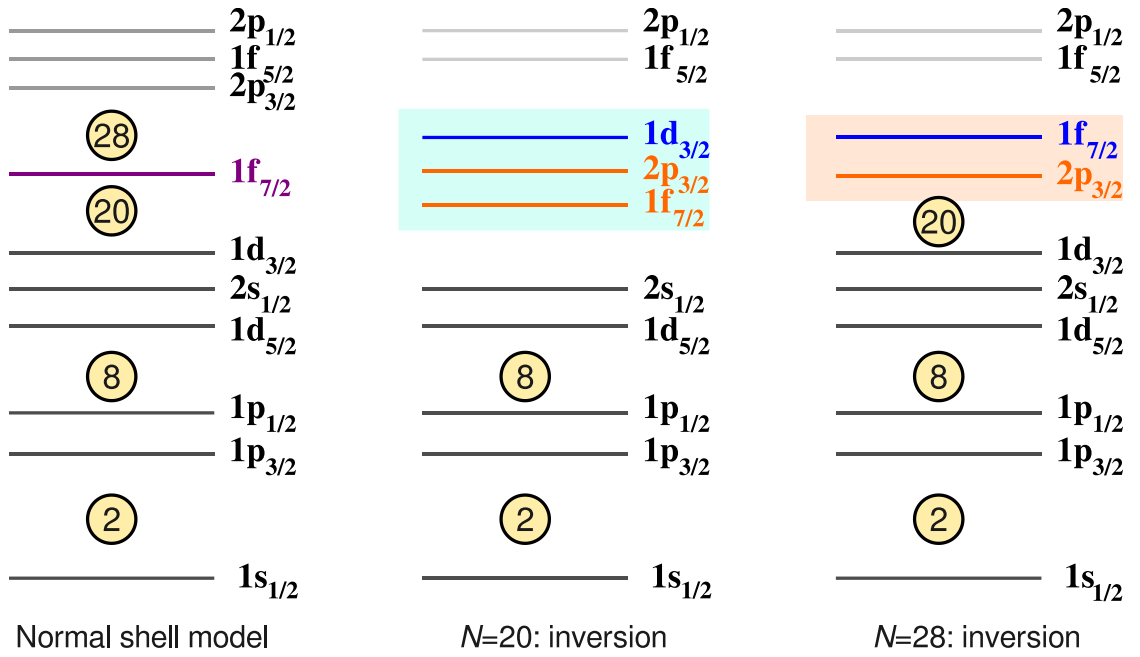

- Recent observation of the disappearance of the **N = 20** shell gap at the low-Z side of the N = 20 chain, led to the identification of the **^{29}F** system as the heaviest known two-neutron Borromean-halo nucleus. *S. Bagchi et al., PRL **124**, 222504 (2020).* ***JS**, JC et. al., PRC **101**, 024310 (2020).* *LF, JC, WH, **JS** et. al., Comm. Physics 3, 132 (2020). JC, **JS**, et. al., PRC **102**, 064227 (2020).*
- Motivated by this observation, it is interesting to explore the low-Z side of the N = 28 shell closure for potential two-neutron Borromean halos in the Na and Mg isotopes.

A. O. Macchiavelli, et al., Eur. Phys. J. A 58, 66 (2022).

- Inversion occur, when energy gap, associated with filling of shell closures disappears.
- Active shells at N = 20 and N = 28 shown with coloured blocks. The $1f_{7/2}$ orbit is bordered by two magic numbers, i.e., 20 and 28.

*E. Caurier et. al., Phys. Rev. C **90** , 014302 (2014).*
*O. Sorlin et. al., PPNP **61** (2), 602–673, (2008).*
*T. Otsuka et. al., Rev. Mod. Phys. **92**, 015002 (2020) .*
***JS**, J. Casal et al., Physics Letters B 853, 138694 (2024).*

Three-Body Structure Model- Hyperspherical framework

PHYSICAL REVIEW C **102**, 064627 (2020)

Three-body Hamiltonian is given by

$$H = T + \sum_{i=1}^{2} V_{core+n_i} + V_{nn} + V_{3b}$$

$$V_{core+n_i} = \left(-V_0 + V_{ls}\vec{l}\cdot\vec{s}\frac{1}{r}\frac{d}{dr}\right)\frac{1}{1+\exp\left(\frac{r-R}{a}\right)}, \qquad V_{3b}(\rho) = v_{3b}e^{-(\rho/\rho_o)^2},$$

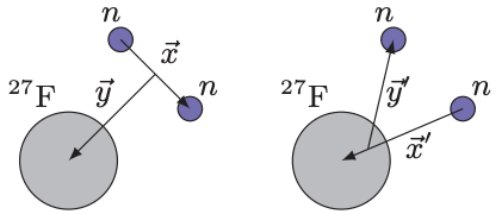

FIG. 1. Jacobi-T (left) and -Y (right) coordinates for the ^{29}F nucleus described as $^{27}\mathrm{F}+n+n$.

nn interaction- Gogny-Pires-Tourreil (GPT) interaction including central, spin-orbit and tensor terms.
*D. Gogny, P. Pires, and R. D. Tourreil, PLB **32**, 591 (1970).*

The three-body force is modelled as a simple Gaussian potential, where $\rho = \sqrt{x^2+y^2}$, is **hyper-radius** and ρ_0=6 fm and the strength v_{3b} is adjusted to recover s_{2n}.

We use the analytical transformed harmonic oscillator (THO) basis, obtained with LST, which changes Gaussian asymptotic behavior of the HO functions into a simple exponential. *J. Casal, M. Rodrguez-Gallardo, and J. M. Arias, Phys. Rev. C **88**, 014327 (2013).*

The diagonalization of the three-body Hamiltonian requires the computation of the corresponding kinetic energy & potential matrix elements**. Spherical inert core approximation is used.**

Reaction cross-section within Glauber model

The reaction cross section for a projectile-target collision integrating the reaction probability with respect to the impact parameter b

$$\sigma_{\mathrm{R}} = \int d\boldsymbol{b}(1 - |\mathrm{e}^{i\chi(\boldsymbol{b})}|^2),$$

Phase shift function

$$\mathrm{e}^{\mathrm{i}\chi(\boldsymbol{b})} = \left\langle \Phi_0^P \Phi_0^T \right| \prod^{A_P} \prod^{A_T} \left[1 - \Gamma_{NN}(\boldsymbol{s}_i^P - \boldsymbol{s}_j^T + \boldsymbol{b})\right] \left| \Phi_0^P \Phi_0^T \right\rangle$$

Profile function

$$\Gamma_{NN}(\boldsymbol{b}) = \frac{1 - i\alpha}{4\pi\beta} \sigma_{NN}^{\mathrm{tot}} \exp\left(-\frac{\boldsymbol{b}^2}{2\beta}\right)$$

PF describes interaction between projectile and target nucleons is expressed as

α, β: determined so as to reproduce the NN scattering

*B. Abu-Ibrahim et al., PRC **77**, 034607 (2008). W. Horiuchi et al., PRC 75, 044607 (2007).*

Phase-shift function: Many-body operator

Approximate using a cumulant expansion: Nucleon-Target profile function

→ Input: **Nuclear density and Profile function no adjustable parameters**

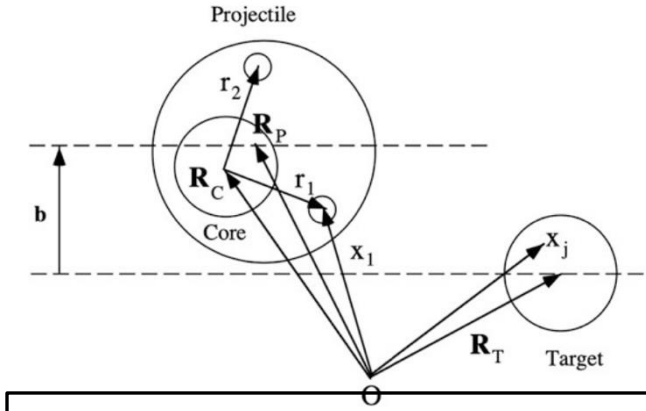

- $\mathbf{r_i = (s_i, z_i)}$ is the coordinate of the two-halo neutron(s) with index i = 1, 2.
- R_C, R_p, and R_T are the position vectors to the COM of the core nucleus, projectile nucleus, and target nucleus, respectively. $x_i - R_C = r_i$.
- s_i and s_j are the two-dimensional vectors of the coordinates for the P and T, measured from their COM which lies on a plane perpendicular to the incident momentum of the projectile

Tale of ^{29}F-I

The University of Manchester

^{29}Ne(-1p) on beryllium target : Exploring the low-Z shore of the Island of Inversion at N = 19

G. Christian et al., PRL 108, 032501 (2012).

Spectroscopy of neutron-unbound ^{27,28}F

*G. Christian et al., PRC **85**, 034327 (2012).*

Two resonance model with lower resonance at **220(50) keV [width =10 keV]** and the upper resonance at **810 keV [width = 100 keV)**

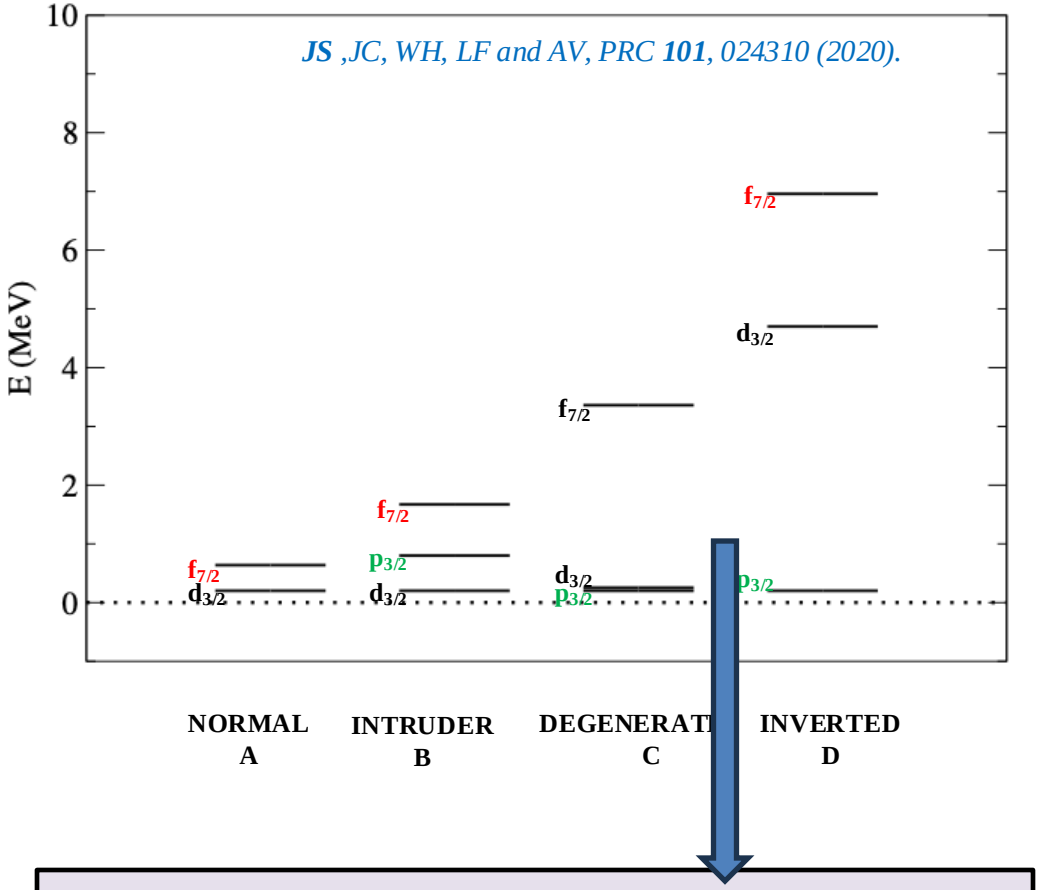

Recently new data arrived

*A. Revel et al., PRL **124**, 152502 (2020).*

The relative-energy spectra and momentum distributions extracted from high precision nucleon-knockout data 29Ne(-1p) and 29F (-1n) showed

-- ground state resonance of ^{28}F at 0.199(6) MeV (l=1~79%)

Inversion !!

-- Ist excited state resonance around 0.966 MeV (l=2~72%)

*JS ,JC, WH, LF and AV, PRC **101**, 024310 (2020).*

Set	S_{2n} (MeV)	$(d_{3/2})^2$	$(f_{7/2})^2$	$(p_{3/2})^2$	R_m (fm)	ΔR (fm)
	0.400	78.7	8.1	9.0	3.363	0.145
	0.790	80.0	8.3	7.9	3.343	0.125
A	1.440	81.3	8.4	6.8	3.323	0.105
	2.090	82.3	8.5	6.0	3.311	0.093
	0.400	43.2	18.0	30.8	3.420	0.202
	0.790	46.8	19.6	26.2	3.380	0.162
B	1.440	50.7	21.1	21.6	3.347	0.129
	2.090	53.4	22.0	18.5	3.329	0.111
	0.400	30.3	5.6	55.7	3.507	0.289
	0.790	37.3	6.5	48.2	3.434	0.216
C	1.440	45.4	7.4	39.8	3.380	0.162
	2.090	51.4	8.0	33.9	3.352	0.134
	0.400	2.8	1.5	87.6	3.598	0.380
	0.790	3.4	1.7	86.7	3.520	0.302
D	1.440	4.2	2.1	85.4	3.459	0.241
	2.090	5.0	2.3	84.2	3.425	0.207

*LF, JC, WH, **JS** and AV, Communication Physics 3, 132 (2020).*

*JC, **JS**, LF, WH and AV, PRC **102**, 064227 (2020).*

Tale of ^{29}F -II

New Experiment confirms ground state resonance of ^{28}F at 0.199(6) MeV (l=1~79%) and Ist excited state resonance around 0.966 MeV (l=2~72%). **Inversion !!**
*A. Revel et al., PRL **124**, 152502 (2020).*

Total reaction Cross section within Glauber Model

The calculated total reaction cross section using the standard Glauber theory are **1370 mb** if we assume s_{2n} = 1.44 MeV, and **1390 mb** if we take the lower limit ($S_{2n} \approx 1$ MeV), which are in good agreement with the observed interaction cross section.

*LF, JC, WH, **JS** and AV, Communication Physics 3, 132 (2020).*

*JC, **JS**, et. al., PRC **102**, 064627 (2020).*

s_{2n} (^{29}F) =1.443 (436) MeV *L. Gaudefroy et al., PRL. 109, 202503 (2012).*

=1.440 (650) MeV *AME 2017.*

Matter radius of ^{29}F

The relative increase of matter radii with respect to ^{27}F core lies in the range **0.20-0.30** fm in the different choices of s_{2n}.

***JS** ,JC, WH, LF and AV, PRC **101**, 024310 (2020).*
*LF, JC, WH, **JS** and AV, Communication Physics 3, 132 (2020).*
*JC, **JS**, LF, WH and AV, PRC **102**, 064227 (2020).*

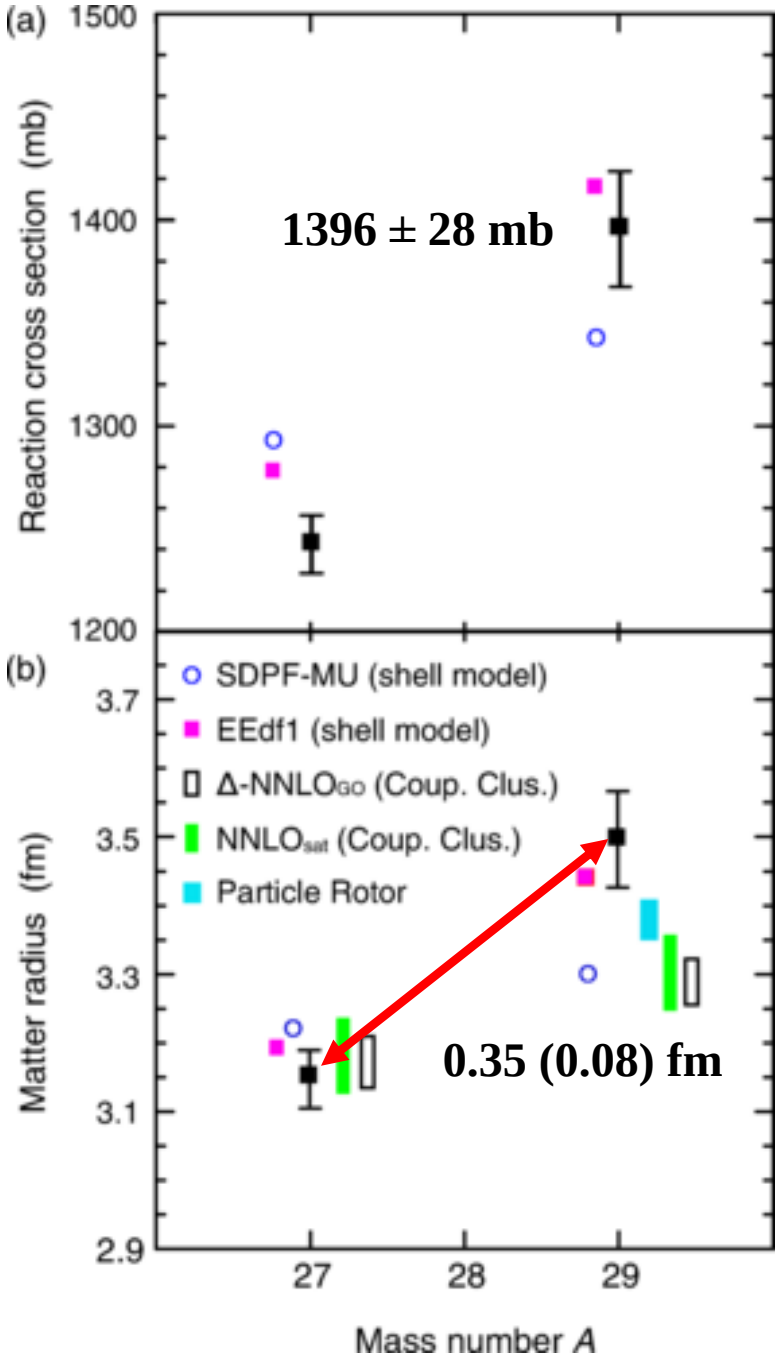

*S. Bagchi et al., PRL **124**, 222504* (2020).

Tale of ^{29}F -III

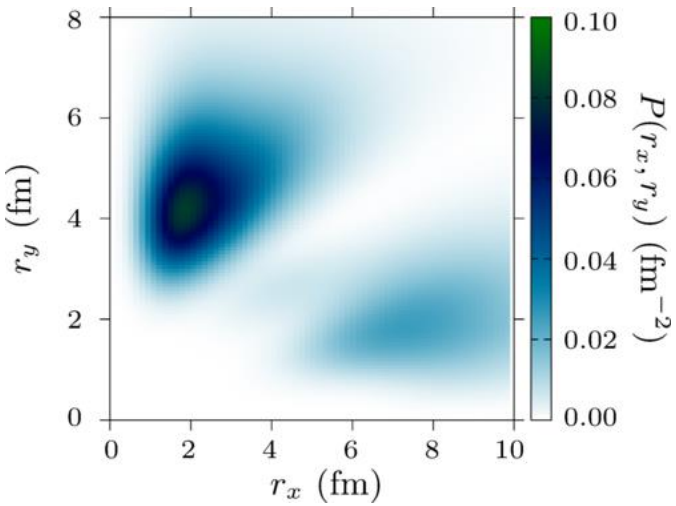

- Ground-state probability density (in fm^{-2}) of ^{29}F using the present three-body model, as a function of $r_x \equiv r_{nn}$ and $r_y \equiv r_{c\text{-}nn}$.
- The large mixing between the $(p_{3/2})^2$ and $(d_{3/2})^2$ components is responsible for the strong dineutron peak and plays a key role in the formation of the two-neutron halo

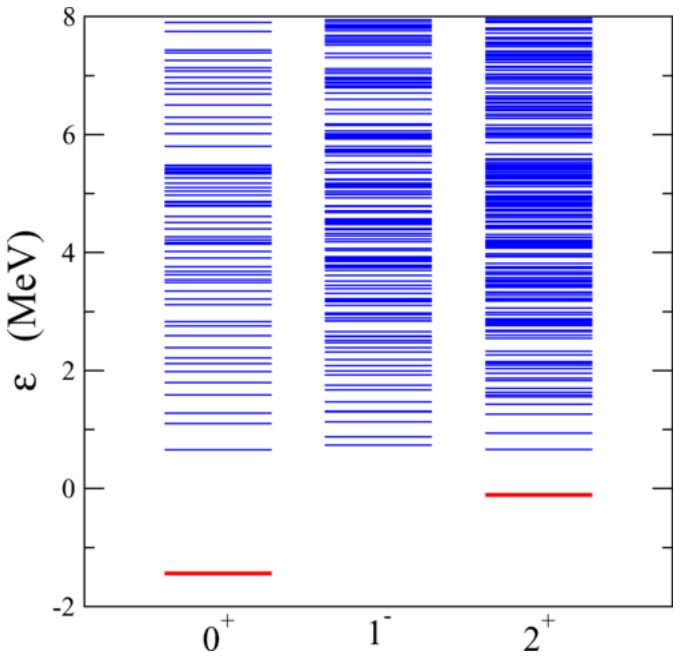

- Energies of the 0+, 1−, and 2+ states of ^{29}F obtained with Pseudo state method.
- Interestingly, the same Hamiltonian produces a very weakly bound 2$^+$ state at E ~0.1 MeV. This energy is not quantitatively consistent with the experimental value, but given the simplicity of the model, the qualitative agreement is remarkable.

*P. Doornenbal, et. al., PRC **95**, 041301(R) (2017).*

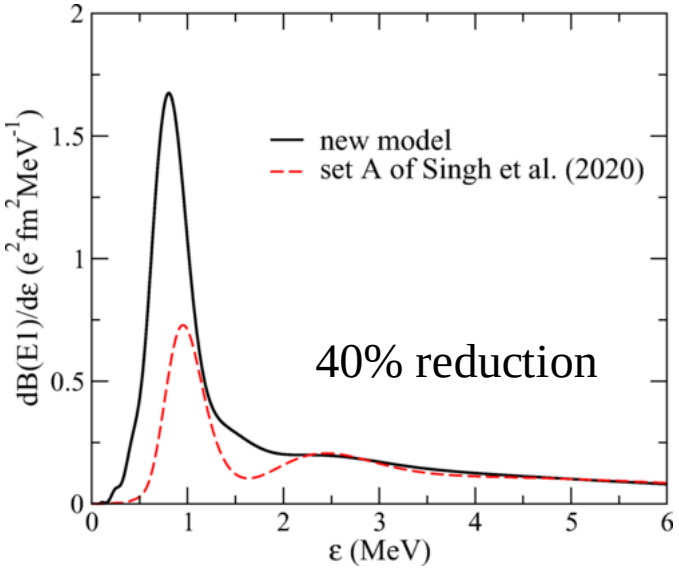

$$B(E\lambda) = |\langle n_0 j_0 || \widehat{O}_{E\lambda} || nj \rangle|^2.$$

- B(E1) distribution obtained in the Inverted scenario (solid black line) compared with the results using the potential set A of Ref. [1] (dashed red line), which corresponds to a standard shell-model order.
- B(E1) distribution is highly sensitive to the ground-state radius and configuration mixing.

*1. **JS** ,JC, WH, LF and AV, PRC **101**, 024310 (2020).*
*2. LF, JC, WH, **JS** and AV, Communication Physics 3, 132 (2020).*
*3. JC, **JS**, LF, WH and AV, PRC **102**, 064227 (2020).*

Two-body (core+n) models for ^{39}Mg and ^{38}Na

K. Fossez, *et. al.*, PHYSICAL REVIEW C **94**, 054302 (2016).
Unbound ground state of ^{39}Mg is predicted to be either a $J^{\pi} = 7/2^-$ or $3/2^-$ state.

A narrow $J^{\pi} = 7/2^-$ or $3/2^-$ ground-state candidate exhibits a resonant structure at 129 KeV.

As we do not have either theoretical or experimental predictions and data for ^{38}Na, we use the same ***core+n*** potential parameters as for ^{39}Mg. The only changes are R_c=1.25A$^{1/3}$and the spin-orbit strength.

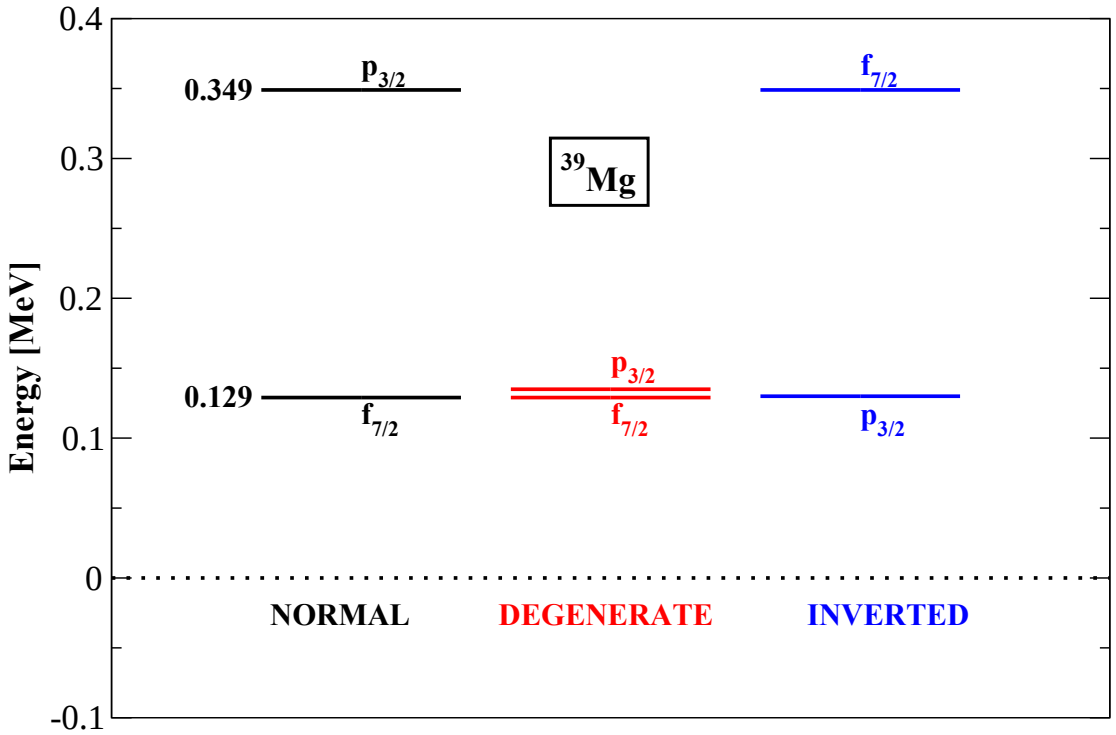

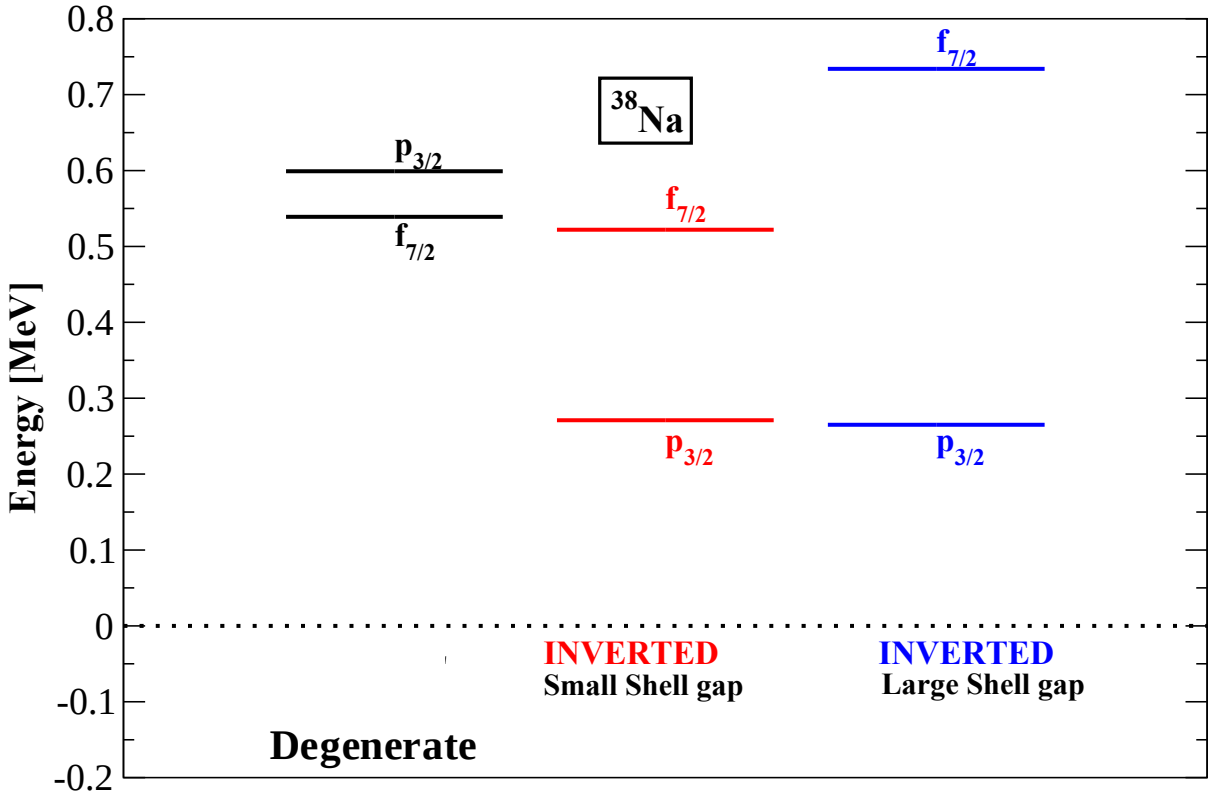

***JS**, J. Casal et al., Physics Letters B 853, 138694 (2024).*

Configuration mixing and matter radii for ^{40}Mg and ^{39}Na

^{40}Mg (s_{2n}) = 0.670 (0.710) MeV
M. Wang, *et. al.*, Chinese Physics C **45 (3)**, 030003 (2021).

Matter radius of core **^{38}Mg**=3.60 fm
S. Watanabe, *et. al.*, PRC **89,** 044610 (2014).

^{39}Na (s_{2n}) = unbound
M. Wang, *et. al.*, Chinese Physics C **45 (3)**, 030003 (2021).
^{39}Na (s_{2n}) = bound (Contradicts AME)
*D. S. Ahn et al., PRL **129**, 212502 (2022).*

Matter radius of core **^{37}Na**=3.64 fm
L. Geng, *et. al.*, NPA **730**, 80 (2004).

Our predictions for s_{2n} of **^{39}Na**
0.010-0.824 (1.828) MeV

The larger change in R_m *w.r.t* core involves wave function which contains significant $(p_{3/2})^2$ (dotted lines) weight, pointing toward the necessity of intruder configurations to sustain halo formation. $(f_{7/2})^2$ (solid lines)

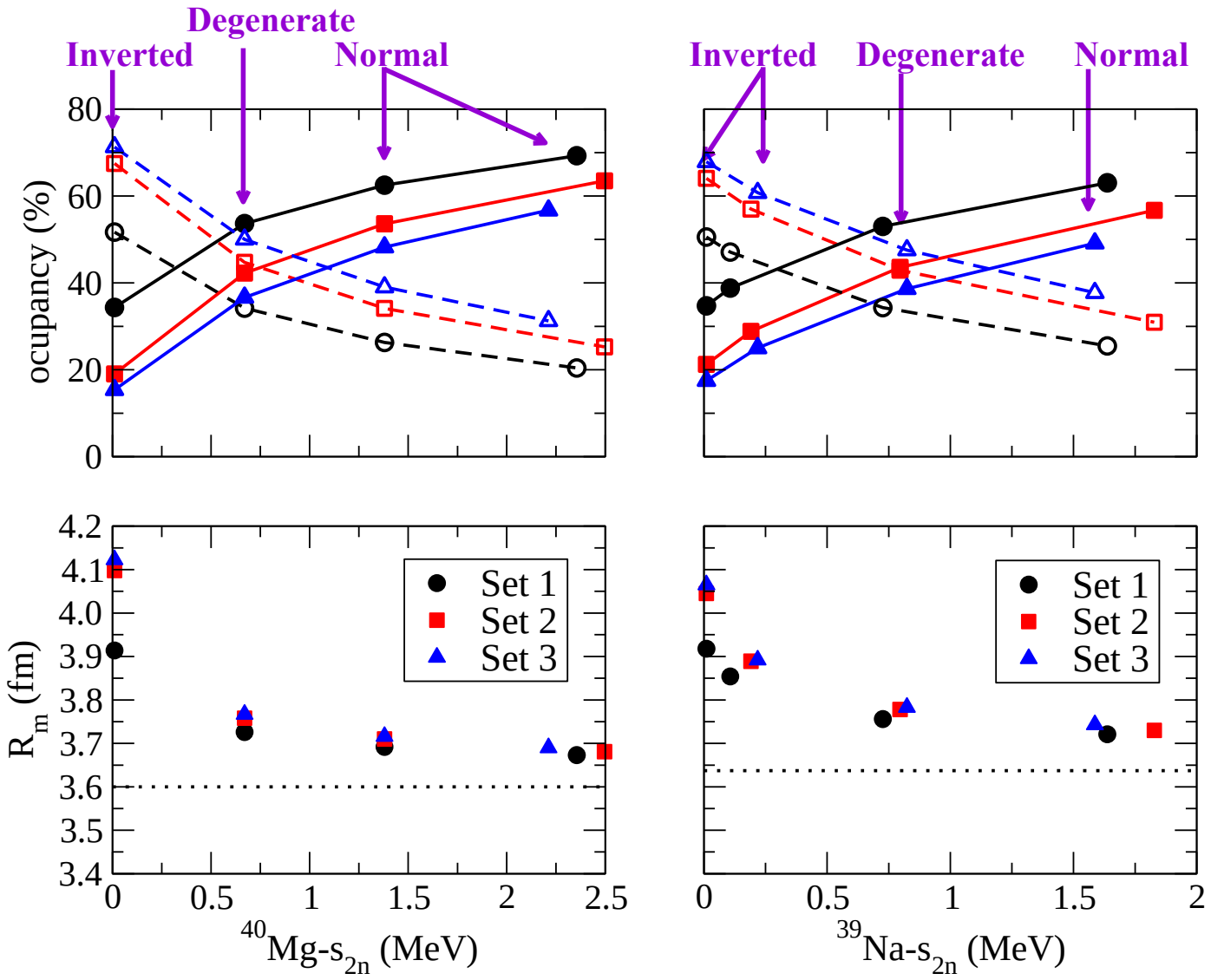

***JS**, J. Casal et al., Physics Letters B 853, 138694 (2024).*

Matter radii for ^{40}Mg and ^{39}Na

- Dotted black lines in the figure correspond to the weighted fit of the experimental data points with the standard $R_0 A^{1/3}$ formula.
- The radii of ^{40}Mg and ^{39}Na are higher than the standard fitted value.
- This observation implies a likely two-neutron halo structure in the ground state of ^{40}Mg and ^{39}Na, and the corresponding melting of the traditional N = 28 shell gap is due to the intrusion of the $p_{3/2}$ orbital.

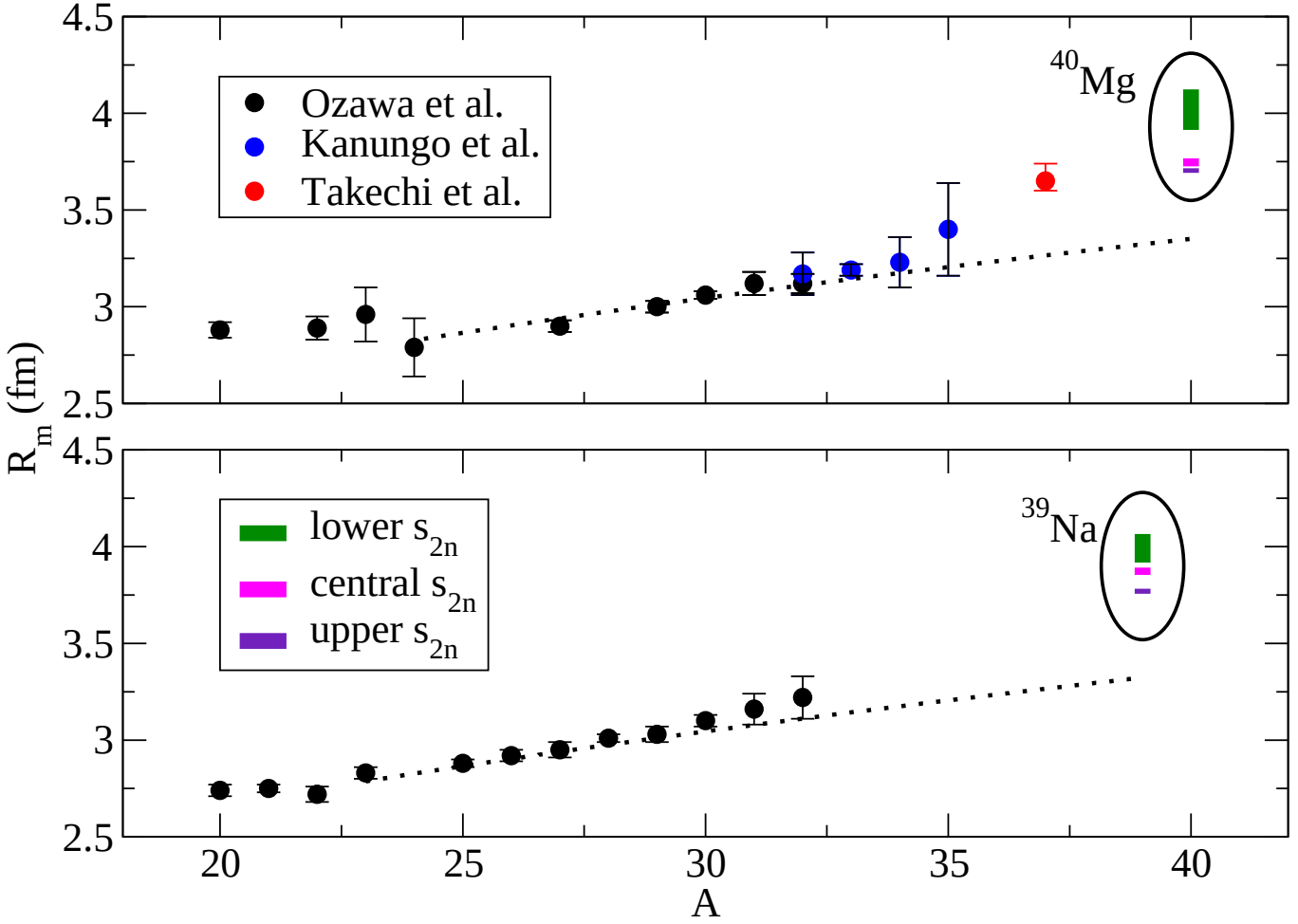

- Ozawa *et al.*, Nuclear Physics A **691 (3)**, 599 (2001).
- Kanungo *et al.*, Phys. Rev. C **83**, 021302 (2011).
- Takechi *et al.*, Phys. Rev. C **90**, 061305(R) (2014).
- ***JS***, *J. Casal et al., Physics Letters B 853, 138694 (2024).*

Reaction cross-sections for ^{40}Mg and ^{39}Na : within Glauber reaction theory

- Experimentally, a very obvious way to determine whether a nucleus is a halo nucleus, is to look for an enhanced reaction cross section. Thus, we examine the total reaction cross section by employing the conventional Glauber theory. *B. Abu-Ibrahim et al., PRC **77**, 034607 (2008). W. Horiuchi et al., PRC 75, 044607 (2007).*

- Using this prescription, we predict the σ_R for ^{40}Mg and ^{39}Na at different incident energies. The predicted values of σ_R for ^{40}Mg and ^{39}Na show significant enhancement with respect to the observed σ_R in the lower-A isotopes for both choices of energy.

Thus, our results provide a clear signal of the 2n-halo structure formation in ^{40}Mg and ^{39}Na and hence melting of the N = 28 shell closure.

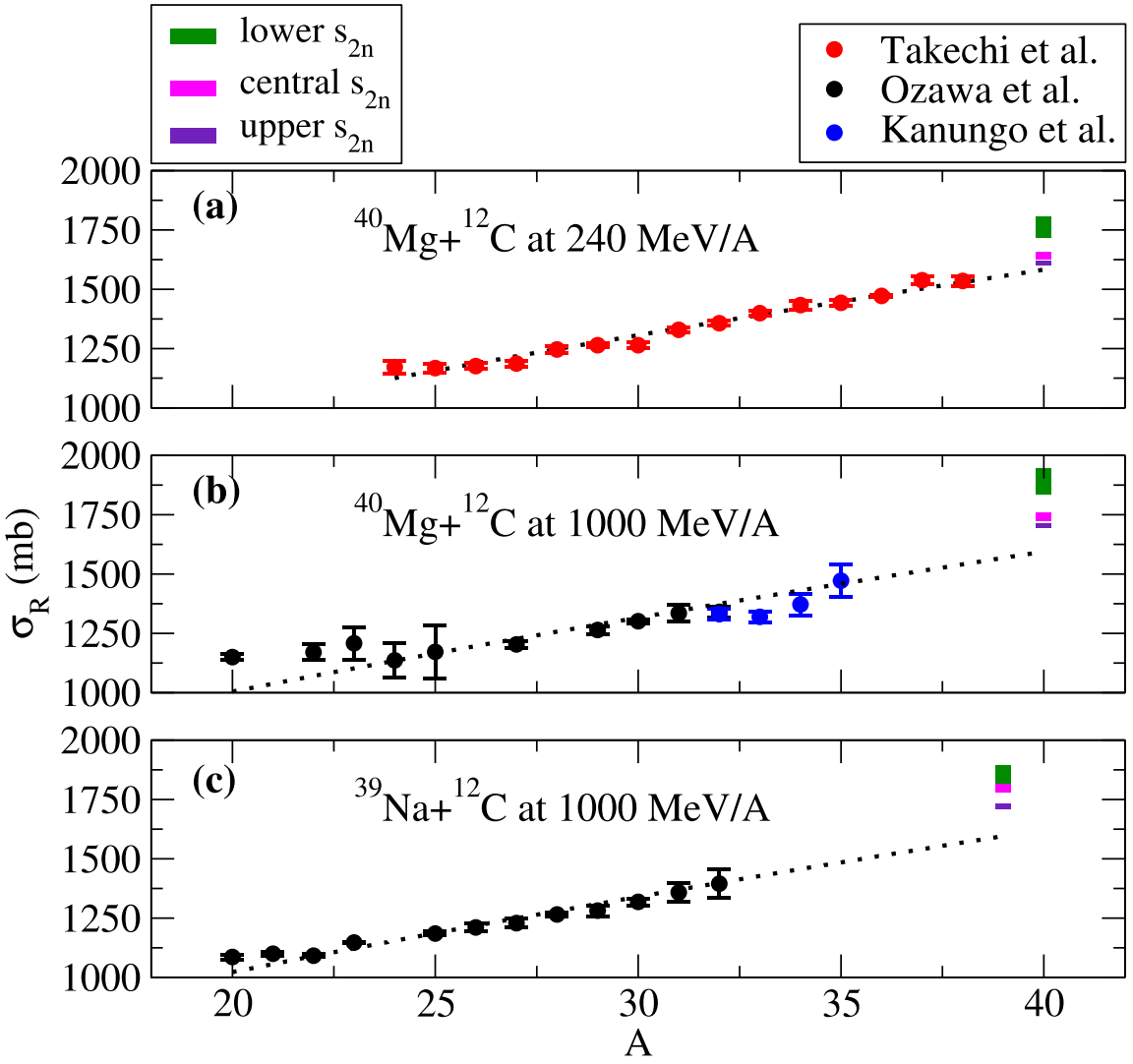

- Ozawa *et al.*, Nuclear Physics A **691 (3)**, 599 (2001).
- Kanungo *et al.*, Phys. Rev. C **83**, 021302 (2011).
- Takechi *et al.*, Phys. Rev. C **90**, 061305(R) (2014).
- ***JS**, J. Casal et al., Physics Letters B 853, 138694 (2024).*

MANCHESTER 1824
The University of Manchester

Summary:

- We started with studying melting of N=20 *(**JS**, JC, WH, LF, and AV, PRC **101**, 024310 (2020))* for ^{29}F. Our results/predictions got boost with new measurements *(S. Bagchi et al., PRL **124**, 222504 (2020) and A. Revel et al., PRL **124**, 152502 (2020)).* We updated our calculations with precise calculations along with detailed analysis of electric-dipole response and reaction calculations *(LF, JC, WH, **JS**, and AV, Commun. Phys. **3**, 132 (2020) and JC, **JS**, LF, WH, and AV, PRC **102**, 064627 (2020)).*
- Motivated by melting N=20 ends up in formation of Borromean in ^{29}F, by using same prescription we reported first three body results for ^{39}Na and ^{40}Mg lying on low-Z side of N=28. *(**JS**, J. Casal et al., Physics Letters B 853, 138694 (2024).*
- Our results calls for new precise mass measurements for s_{2n} of three-body systems and the low-lying continuum spectrum of two-body subsystems to better constrain the theoretical models.
- The disappearance of the conventional N=28 shell gap and emergence of the halo leads to significant occupancy of intruder $p_{3/2}$ orbit in the ground state of ^{39}Na and ^{40}Mg. Nevertheless, it is imperative to verify this conclusion through experimental measurements of interaction cross sections and transfer or knock out data to probe partial-wave content.

Future Perspectives:

- It is interesting to see how our predictions are affected with inclusion of core deformation effects.

  H. H. Li et al., PHYSICAL REVIEW C 109, L061304 (2024)
- Calculation of electric dipole (E1) response for ^{39}Na and ^{40}Mg .

MANCHESTER 1824
The University of Manchester

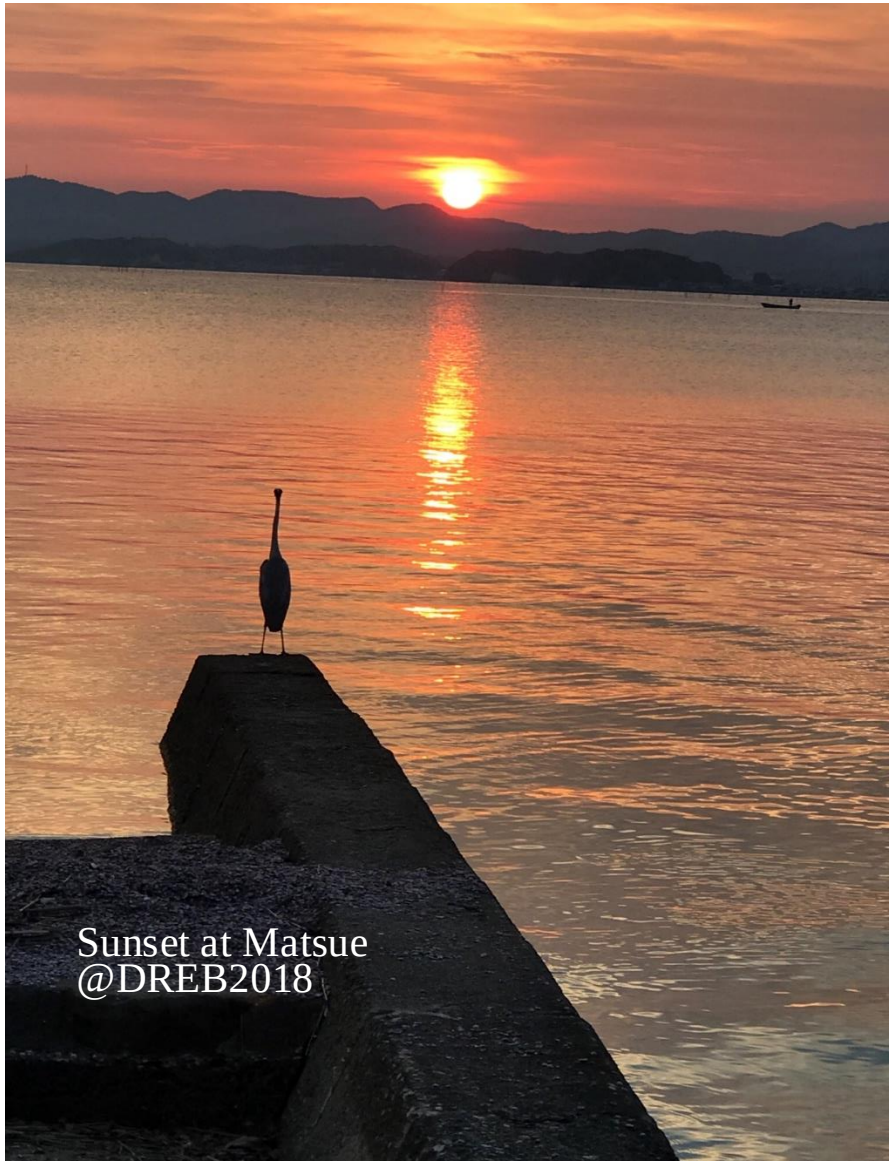

Thanks for kind attention.

Acknowledgements:

J. Casal (Seville)
W. Horiuchi (OMU, Osaka)
N. R. Walet (Manchester)
W. Satula (Warsaw)
L. Fortunato (Padova)
A. Vitturi (Padova)

MANCHESTER 1824
The University of Manchester

2n-density of ^{40}Mg

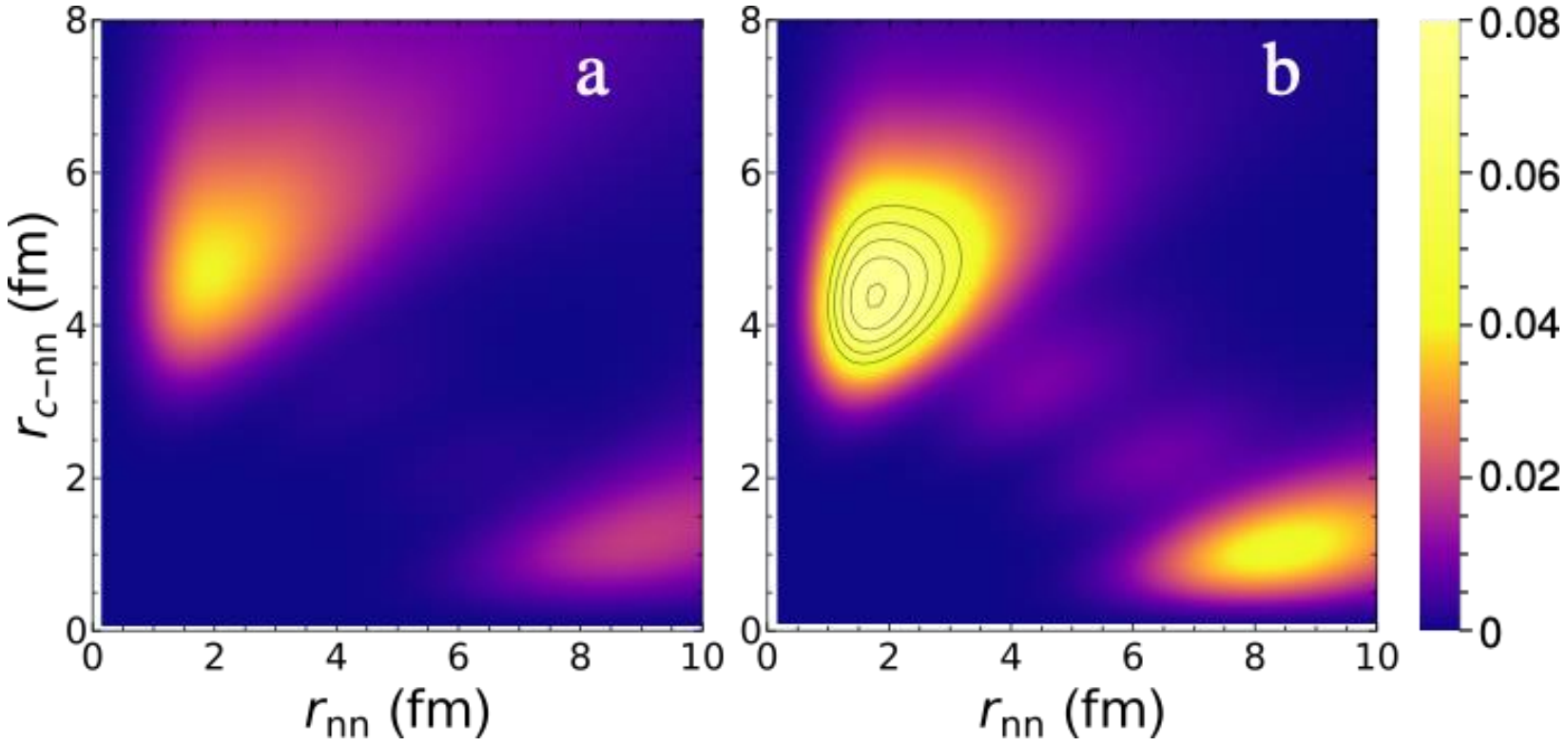

The ground state probability density distribution (in units of fm^{-2}) for ^{40}Mg for Set-3 (a) with s_{2n} =- 0.010 MeV and (b) with s_{2n} = -1.380 MeV. The contour lines in (b) show the shape of the peak above a probability of 0.04, which is twice as high as that in (a).